

Contact Chemistry and Single-Molecule Conductance: A Comparison of Phosphines, Methyl Sulfides, and Amines

Young S. Park,^{†,§} Adam C. Whalley,^{†,§} Maria Kamenetska,^{‡,§} Michael L. Steigerwald,[†]
Mark S. Hybertsen,^{§,¶} Colin Nuckolls,^{†,§} and Latha Venkataraman*^{‡,§}

Department of Chemistry, Department of Applied Physics and Applied Mathematics, and Center for Electron Transport in Molecular Nanostructures, Columbia University, New York, New York 10027, and Center for Functional Nanomaterials, Brookhaven National Laboratory, Upton, New York 11973

Received September 28, 2007; E-mail: lv2117@columbia.edu

Understanding the transport characteristics of single molecules bonded between metal electrodes is of fundamental importance for molecular scale electronics.¹ It is well-known that these characteristics are influenced by intrinsic molecular properties such as their length, conformation, gap between the highest occupied and lowest unoccupied molecular orbitals, and the alignment of this gap to the metal Fermi level.² Here we show that transport through single-molecule junctions also depends on the nature of the chemical linker group used to bind molecules to metal electrodes. We compare the low bias conductance of a series of alkanes terminated on their ends with dimethyl phosphines, methyl sulfides, and amines and find that junctions formed with dimethyl phosphine terminated alkanes have the highest conductance. Furthermore, we see a clear conductance signature with these linker groups, indicating that the binding is well-defined and electronically selective.

We recently showed that conductance measurements of single-molecule junctions formed using gold metal electrodes become reliable and reproducible when amine link groups are used.³ Junctions are created by repeatedly forming and breaking Au point contacts⁴ with a modified STM in a solution of the molecules in 1,2,4-trichlorobenzene (Figure 1A).

Figure 1B compares individual conductance traces for an *n*-butyl group terminated on each end with either amines (NH₂), dimethyl phosphines (PMe₂), or methyl sulfides (SMe). These molecules and others used in this study were either commercially available or prepared by known methods.⁵ The traces reveal steps at molecule-dependent conductance values below G_0 , the quantum of conductance, that are due to conduction through a molecule bonded in the gap between the two Au point contacts. Repeated measurements give a statistical assessment of the junction properties. Figure 2A shows the conductance histograms generated, without any data selection, from thousands of consecutively measured conductance traces. The histograms reveal an unambiguous peak for all the molecules measured. By fitting this peak to a Lorentzian function, we can determine the most probable conductance value for the junctions.

The most probable conductance for the three different link groups for the alkanes tested is shown in Figure 2B. The data reveal that the conductance (G) decreases exponentially with increasing molecular length (L) with $G \sim \exp(-\beta L)$. The tunneling decay constant, β (per CH₂ group), determined from the fit to the conductance data (Figure 2B) is 0.93 ± 0.02 for NH₂, 0.89 ± 0.04 for SMe, and 1.02 ± 0.02 for PMe₂ link groups. These small differences in β for these three link groups could originate from a

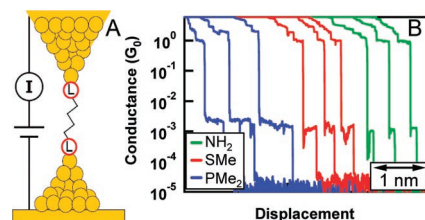


Figure 1. (A) Cartoon of measurement, with L indicating the ligand position on the alkane backbone. (B) Sample conductance traces measured while breaking gold point contacts in a solution of butane with terminally substituted PMe₂ (blue), SMe (red), or NH₂ (green) link groups.

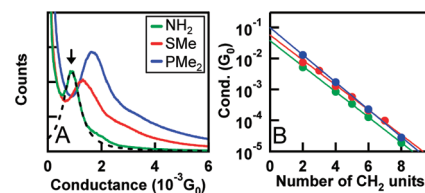


Figure 2. (A) Conductance histograms generated without data selection from over 34 000 consecutively measured traces for an *n*-butyl group terminated on each end with NH₂ (green), PMe₂ (blue), or SMe (red). Histogram bin size is $10^{-5} G_0$ for all traces. The peaks are determined from Lorentzian fits as shown for butanediamine (black dashed line). (B) Conductance of all alkanes plotted against the number of methylene groups in the chain shown on a semilog scale. Also shown are the linear fits to the data on the semilog scale.

difference in Fermi level alignment within the HOMO–LUMO gap of the molecules and small differences in the charge transfer between the ligand lone pair and the Au contacts. We can estimate an “effective contact resistance” for each link group by extending the fits to zero CH₂ units since the conduction mechanism is through nonresonant tunneling.⁶ We find that the PMe₂ link group has the lowest effective contact resistance of 130 k Ω , significantly lower than that of the SMe (270 k Ω) and NH₂ links (370 k Ω).

When a single-molecule junction, as illustrated in Figure 1A, is pulled, it will break at the weakest link, which could be at either the molecule–gold bond or a gold–gold bond. In order to determine the average distance a single-molecule junction can be extended before the junction breaks, we examined step-length data in more detail. Figure 3 shows an analysis of large data sets (> 34 000 traces each) obtained for *n*-butyl bridges that are terminated with PMe₂, SMe, or NH₂ groups. We use an automated algorithm⁷ to determine, for each measured trace, the length of the molecular step, and we show the distributions of step lengths in Figure 3A (see Supporting Information). We find that 50% of the traces have steps longer than 0.8 Å for NH₂ links, 1.7 Å for the SMe links, and 3.2 Å for the PMe₂ links.

[†] Department of Chemistry, Columbia University.

[‡] Department of Applied Physics and Applied Mathematics, Columbia University.

[§] Center for Electron Transport in Molecular Nanostructures, Columbia University.

[¶] Brookhaven National Laboratory.

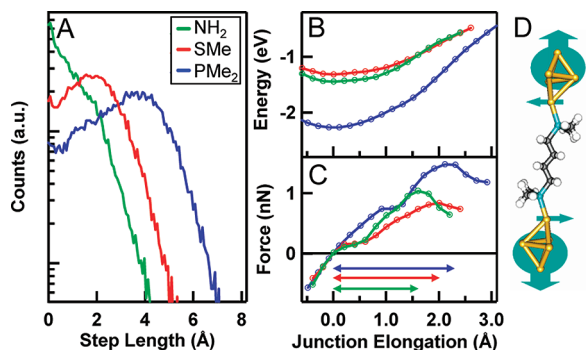


Figure 3. (A) Step-length histograms showing the distribution of lengths that molecular junctions of butane with PMe_2 (blue), SMe (red), and NH_2 (green) link groups can be extended. Step-length distributions are determined by an automated algorithm. Calculated junction formation energy for two L–Au bonds (B) and applied force (C) versus elongation of model junctions of the three molecules shown in A. (D) Illustration for butane with PMe_2 links shown with 1.4 Å elongation. Gold clusters represent the undercoordinated Au contact atom and its environment. The junction is elongated by stepwise displacing the four highlighted Au atoms on each side, allowing full relaxation of all other atoms.

What is the origin of these large differences in the step length distributions for different end groups? To help answer this question, we have performed density functional theory (DFT)-based calculations⁸ for the *n*-butyl molecules bound to Au clusters (see Supporting Information). We find that a donor–acceptor bond is formed through the delocalization of the lone pair on the phosphorus in PMe_2 and the sulfur in SMe to an undercoordinated gold atom as we had previously shown for the amine link group.³ The unambiguous peak seen in our data for all three ligands indicates that this donor–acceptor bond is both selective and well-defined. We find that the Au– NH_2R and Au– SMeR bonds have similar strengths around 0.6 eV, while the Au– PMe_2R bond is significantly stronger (~1.2 eV), suggesting that the binding energies alone do not explain the step-length distributions.

In a computational experiment, the junctions were elongated stepwise, allowing the Au contact atoms and the molecule to relax fully at each step. The resulting junction energy curves and their derivatives that measure the force applied to the junction at each step are shown in Figure 3B and C. In each case, at the point of maximum force, the donor–acceptor bond is elongated and each contact Au atom begins to relax back toward its parent Au_4 cluster. This implies that the junctions break at a ligand–Au bond. The calculated maximum force is less than or comparable to the measured breaking force in Au point contacts (1.5 nN).⁹ The elongation from the energy minimum to the force maximum systematically increases from NH_2 to SMe to PMe_2 (represented by horizontal arrows in Figure 3C), consistent with trends in orbital size and the measured step-length histogram trends. Interestingly, the force curves all show a flattening at smaller elongation that corresponds to the point at which the contact Au atom shifts laterally (arrows in Figure 3D). The force and energy required to shear the undercoordinated Au atom from a hollow to a bridge site are small: this is a soft degree of freedom in the junction. The donor–acceptor bonds discussed here are thus strong enough to move the contact Au atoms; this surface-atom mobility is one source of the long steps seen here. Stronger ligand–metal bonds lead to more metal–surface distortion; therefore, the junctions using phosphine bridges give the longest steps. However, the size and shape of the

lone-pair orbital on the ligand also affect the step lengths. Larger more diffused orbitals give bonds with weaker force constants; thus, the SMe ligand gives significantly longer steps than the NH_2 , even though the two bond strengths are roughly equal.

We have shown that the donor–acceptor bonds between these ligands and gold result in selective bonding that provides an unambiguous conductance signature for single-molecule junctions. The σ -donation from the lone pair to the metal is strongest for the phosphines, followed by the amines, and weakest for the sulfides, while π -back-donation from the metal to the ligand is known to be more significant in phosphines than in sulfides than in amines.¹⁰ The trend in the calculated bond strength reflects the balance of these processes. We have successfully explained trends in the conductance through amine–gold-linked molecules as mediated by Au *s*–N lone-pair σ -states.³ We hypothesize that the increased availability of ligand d states in sulfides and phosphines leads to a π -channel for electron transfer through the SMe- and PMe_2 -linked junctions. This additional channel accounts for the trends seen in the contact resistance. In particular, the strongest role for π -back-donation in the phosphines corresponds to the increased conductivity seen for phosphines compared with methyl sulfides and amines.

In summary, we have shown that the link group is a rich area for study of molecular conductance. We find that trialkyl phosphines have extremely sharp conductance histograms and have the lowest contact resistance. These results augur well for the preparation of new types of linkages that go beyond donor–acceptor bonds to form electrically transparent contacts.

Acknowledgment. This work was supported primarily by the Nanoscale Science and Engineering Initiative of the National Science Foundation (NSF) under NSF award number CHE-0641523 and by the New York State Office of Science, Technology, and Academic Research (NYSTAR). This work was supported in part by the U.S. Department of Energy, Office of Basic Energy Sciences, under contract number DE-AC02-98CH10886. M.L.S. thanks the MRSEC Program of the NSF under award number DMR-0213574.

Supporting Information Available: Synthesis procedures, data analysis, and theoretical methods. This material is available free of charge via the Internet at <http://pubs.acs.org>.

References

- (1) (a) Nitzan, A.; Ratner, M. A. *Science* **2003**, *300* (5624), 1384–1389. (b) Joachim, C.; Ratner, M. A. *Proc. Natl. Acad. Sci. U.S.A.* **2005**, *102* (25), 8800–8800.
- (2) Salomon, A.; Cahen, D.; Lindsay, S.; Tomfohr, J.; Engelkes, V. B.; Frisbie, C. D. *Adv. Mater.* **2003**, *15* (22), 1881–1890.
- (3) (a) Venkataraman, L.; Klare, J. E.; Tam, I. W.; Nuckolls, C.; Hybertsen, M. S.; Steigerwald, M. L. *Nano Lett.* **2006**, *6* (3), 458–462. (b) Venkataraman, L.; Klare, J. E.; Nuckolls, C.; Hybertsen, M. S.; Steigerwald, M. L. *Nature* **2006**, *442* (7105), 904–907.
- (4) Xu, B. Q.; Tao, N. J. *Science* **2003**, *301* (5637), 1221–1223.
- (5) (a) Pindzola, B. A.; Jin, J. Z.; Gin, D. L. *J. Am. Chem. Soc.* **2003**, *125* (10), 2940–2949. (b) Anklam, E. *Synthesis* **1987**, (9), 841–843.
- (6) (a) Beebe, J. M.; Engelkes, V. B.; Miller, L. L.; Frisbie, C. D. *J. Am. Chem. Soc.* **2002**, *124* (38), 11268–11269. (b) Chen, F.; Li, X. L.; Hihath, J.; Huang, Z. F.; Tao, N. J. *J. Am. Chem. Soc.* **2006**, *128* (49), 15874–15881.
- (7) Quek, S. Y.; Venkataraman, L.; Choi, H. J.; Louie, S. G.; Hybertsen, M. S.; Neaton, J. B. *Nano Lett.* **2007**, *7* (11), 3477–3482.
- (8) (a) *Jaguar 5.0*; Schrödinger, LLC: Portland, OR, 1991–2003. (b) Perdew, J. P.; Burke, K.; Ernzerhof, M. *Phys. Rev. Lett.* **1996**, *77* (18), 3865–3868. (c) Wadt, W. R.; Hay, P. J. *J. Chem. Phys.* **1985**, *82* (1), 284–298.
- (9) Rubio, G.; Agrait, N.; Vieira, S. *Phys. Rev. Lett.* **1996**, *76* (13), 2302–2305.
- (10) Collman, J. P.; Hegedus, L. S.; Norton, J. R.; Finke, R. G. *Principles and Applications of Organotransition Metal Chemistry*; University Science Books: Mill Valley, CA, 1987.

JA0773857